

# Puerto Rico Historical Climate Analysis

---

*A closer look at complex tropical terrain*

**Environmental Science Division**

### **About Argonne National Laboratory**

Argonne is a U.S. Department of Energy laboratory managed by UChicago Argonne, LLC under contract DE-AC02-06CH11357. The Laboratory's main facility is outside Chicago, at 9700 South Cass Avenue, Lemont, Illinois 60439. For information about Argonne and its pioneering science and technology programs, see [www.anl.gov](http://www.anl.gov).

### **DOCUMENT AVAILABILITY**

**Online Access:** U.S. Department of Energy (DOE) reports produced after 1991 and a growing number of pre-1991 documents are available free at OSTI.GOV (<http://www.osti.gov/>), a service of the US Dept. of Energy's Office of Scientific and Technical Information.

### **Reports not in digital format may be purchased by the public from the National Technical Information Service (NTIS):**

U.S. Department of Commerce  
National Technical Information Service  
5301 Shawnee Rd  
Alexandria, VA 22312

**[www.ntis.gov](http://www.ntis.gov)**

Phone: (800) 553-NTIS (6847) or (703) 605-6000

Fax: (703) 605-6900

Email: [orders@ntis.gov](mailto:orders@ntis.gov)

### **Reports not in digital format are available to DOE and DOE contractors from the Office of Scientific and Technical Information (OSTI):**

U.S. Department of Energy  
Office of Scientific and Technical Information  
P.O. Box 62  
Oak Ridge, TN 37831-0062

**[www.osti.gov](http://www.osti.gov)**

Phone: (865) 576-8401

Fax: (865) 576-5728

Email: [reports@osti.gov](mailto:reports@osti.gov)

### **Disclaimer**

This report was prepared as an account of work sponsored by an agency of the United States Government. Neither the United States Government nor any agency thereof, nor UChicago Argonne, LLC, nor any of their employees or officers, makes any warranty, express or implied, or assumes any legal liability or responsibility for the accuracy, completeness, or usefulness of any information, apparatus, product, or process disclosed, or represents that its use would not infringe privately owned rights. Reference herein to any specific commercial product, process, or service by trade name, trademark, manufacturer, or otherwise, does not necessarily constitute or imply its endorsement, recommendation, or favoring by the United States Government or any agency thereof. The views and opinions of document authors expressed herein do not necessarily state or reflect those of the United States Government or any agency thereof, Argonne National Laboratory, or UChicago Argonne, LLC.

**ANL-23/09**

## **Puerto Rico Historical Climate Analysis**

---

*A closer look at complex tropical terrain*

prepared by  
Kenny Puleikis and Jiali Wang  
Environmental Science Division, Argonne National Laboratory

May 2023



## CONTENTS

ABSTRACT.....	5
1 INTRODUCTION.....	6
2 DATA.....	7
2.1 Daymet Version 4.....	7
2.2 ERA5.....	8
2.3 Station Observations.....	9
3 METHOD.....	9
4 RESULTS.....	9
4.1 Temperature.....	10
4.2 Precipitation.....	14
4.3 Shortwave Radiation.....	18
4.4 Large-Scale Meteorological Conditions.....	19
4.5 Local-Scale Land Cover Changes.....	22
5 SUMMARY AND DISCUSSION.....	22
6 ACKNOWLEDGEMENTS.....	23
7 DATA AVAILABILITY.....	23
8 REFERENCES.....	23

## FIGURES

1. Terrain map of Puerto Rico including elevation and sites of observation data used in this report.....	7
2. 1950-2019 averaged fall air temperature using standard ERA5 atmosphere (spatial resolution: 30 km, top), and ERA5 land-only (spatial resolution: 9 km, bottom).....	8
3. (a) Seasonal mean temperature in Fahrenheit, 1950–2019. (b) Seasonal mean difference in Fahrenheit, 1989–2019 minus 1950–1979. (c) Long-term trend (or slope of linear regression) of seasonal mean temperature, 1950–2019.....	10

**FIGURES (CONT.)**

4. (a) Seasonal average daily maximum air temperature in summer, spring, and fall, and daily minimum air temperature in winter. (b) Air temperature difference between 1989–2019 and 1950–1979 (1989–2019 minus 1950–1979) for seasonal average maximum of summer, spring, and fall and minimum of winter. (c) Long-term trend (or slope of linear regression) of seasonal maximum temperatures for summer, spring, and fall and seasonal minimum for winter, 1950–2019. ....12

5. Daymet and in-situ observed 2-m air temperature (in Fahrenheit) time-series in summer and winter over Coloso (Northwest), San Juan (Northeast), Lajas (Southwest), Guayama (Southeast), Adjuntas (western mountain), and Aibonito (eastern mountain). Solid lines are Daymet, dashed lines are in-situ observations.....13

6. Daymet precipitation data with observation sites. (a) Seasonal mean daily precipitation (mm/day), 1950–2019. (b) Seasonal percentage change of averaged daily precipitation, 1989–2019 minus 1950–1979. (c) Long-term trend (or slope of linear regression) of seasonal averaged daily precipitation, 1950–2019. ....15

7. Long-term trend (or slope of linear regression) of seasonal precipitation change with respect to year from 1950-2019 (mm/yr). ....15

8. Time series of daily precipitation (in mm/day) for Coloso, San Juan area, Adjuntas, Aibonito, Lajas, and Guayama for fall (the wettest season) during 1950–2019 for Daymet and even longer time series for certain locations. Solid lines are based on Daymet data. Dashed lines are based on station observations. ....16

9. Daymet extreme precipitation data with observation sites. (a) Percentage change of seasonal 95th percentile daily precipitation in 1950–1979 compared to 1989–2019. (b) Percentage change of seasonal 5th percentile daily precipitation in 1950–1979 compared to 1989–2019. ....17

10. Daymet shortwave radiation data with observation sites: (a) Seasonal mean incident shortwave radiation in  $W/m^2$  per daylight hour, 1950–2019. (b) Seasonal difference of shortwave radiation in  $W/m^2$ , 1989–2019 minus 1950–1979. (c) Long-term trend of seasonal shortwave radiation, 1950–2019. ....19

11. Top: Changes in ERA5 monthly averaged SLP. Bottom: Changes in total cloud cover. Changes are calculated using the 1999–2019 average minus the 1959–1979 average. ....20

12. ERA5 monthly averaged TCRW. Top: Average monthly TCRW in  $kg/m^2$  from 1959–2019. Bottom: Changes in monthly averaged TCRW, 1999–2019 average minus 1959–1979 average.....20

13. (a) ERA5 seasonally averaged 10-m wind speeds (contours) and directions (arrows), 1959–2019. (b) Changes in winds in each season, 1959–1979 compared to 1999–2019 (1999–2019 minus 1959–1979).....21

## ABSTRACT

Small tropical islands like Puerto Rico are especially vulnerable to climate change impacts, yet are often underrepresented in most datasets because the spatial resolution is too coarse to sufficiently cover their complex terrain. This study was done to better understand how the climate has changed in the various regions of Puerto Rico, which will support a transition to renewable energy and aid in projecting future climate impacts on the residents and land they live on. This study used multiple datasets including Daymet, a daily surface weather and climatological summary; European Centre for Medium-Range Weather Forecasts Reanalysis version 5 (ERA5); and station observations. The climate variables examined here include minimum and maximum near-surface air temperature, daily precipitation, incident shortwave radiation, and large-scale upper atmosphere conditions. The time periods cover the years 1950–2019. Results in both Daymet and station observations show long-term warming trends throughout every season. In particular, the minimum winter temperatures increased the most compared with maximum and mean air temperature. Northeast Puerto Rico, where the majority of the island’s population is located, experienced the largest warming. Summertime precipitation has decreased over time, and spring and fall precipitation has increased. The largest increase in fall is because there has been more available precipitable water, lower sea-level pressure, and favorable cyclonic circulations from the trade winds over the past seven decades. Overall, wet days are getting wetter, while dry days are getting drier. While there are good solar energy potential, we see a long-term decreasing trend in shortwave radiation over time in all seasons across entire island, possibly due to the increase of cloud cover.

# 1 INTRODUCTION

Small tropical islands are vulnerable to the impacts of climate change. These impacts include increased dry periods, lower productivity in food and products, decreased local biodiversity, and an overall rise in sea levels, which can affect the livability of low-elevation coastal regions (Fordham and Brook 2010; Singh and Bainsla 2015). Puerto Rico is uniquely vulnerable even among tropical islands, due to its low-lying geography, hydrological landscape, and small size (Ramos-Scharrón et al. 2021). The impacts of climate change are also found to increase the intensity of tropical storms in the region based on observations (e.g., Kang and Elsner 2015; Bhatia et al. 2019). These extreme storms have extensive impacts on Puerto Rico’s property and power grid. In 2017, for example, Hurricane Maria caused an estimated 2,982 fatalities and the largest blackout in U.S. history, and left 1.5 million people without power and over \$90 billion in property damages (Pasch et al. 2023). Although Puerto Rico is a U.S. territory, climate observations over the region are not as extensive as data available over the contiguous United States (CONUS). Many regional climate models have spatial resolutions that are too coarse to cover the complex terrain of Puerto Rico, and some do not attempt to cover the small island at all (Mearns et al. 2017; Liu et al. 2017; Gensini et al. 2023). Global climate models or earth system models that have grid spacing coarser than 2 degrees have even worse difficulties; they may completely ignore the island and treat it as an ocean grid.

Puerto Rico is largely composed of mountains that span west–east on the interior of the island, with steeper slopes to the south (Figure 1). In the mountains, Adjuntas is sparsely populated while the other coastal cities have much larger populations. The most densely populated areas are the lowlands on the northern coast and a few regions of lowlands along the southern and western coasts. Puerto Rico had a population of 3.194 million in 2020, in stark contrast to only 2.205 million in 1950—a 44.85% increase in population over the 70 years. San Juan, the capital of Puerto Rico, is located in these northern lowlands. It has the highest population in Puerto Rico, roughly 342,259 inhabitants as of 2020. It has grown from nearly 224,000 in 1950. The San Juan metro area, which consists of San Juan and much of the eastern half of the island, is roughly 76% of Puerto Rico’s entire population. The lowlands are also used as farmland, making them especially vulnerable to temperature and water changes within the regions. Existing studies of the region tend to focus on specific events, because the island is heavily affected by extreme storms such as hurricanes (Pokhrel et al. 2021). Climate change has only worsened these extreme events (e.g., Bhatia et al. 2019). To make informed decisions on infrastructure going forward, it is important to understand how Puerto Rico’s climate has changed in observable history. Renewable energy on the island would mitigate climate change impacts in the region and make the power grid less vulnerable in cases of extreme events. This report utilizes unique observation-based and reanalysis data products and provides a look into long-term historical climate change impacts on prevalent weather variables. It also explains the changes of these variables due to large scale environment change such as sea level pressure, precipitable water, as well as trade winds.

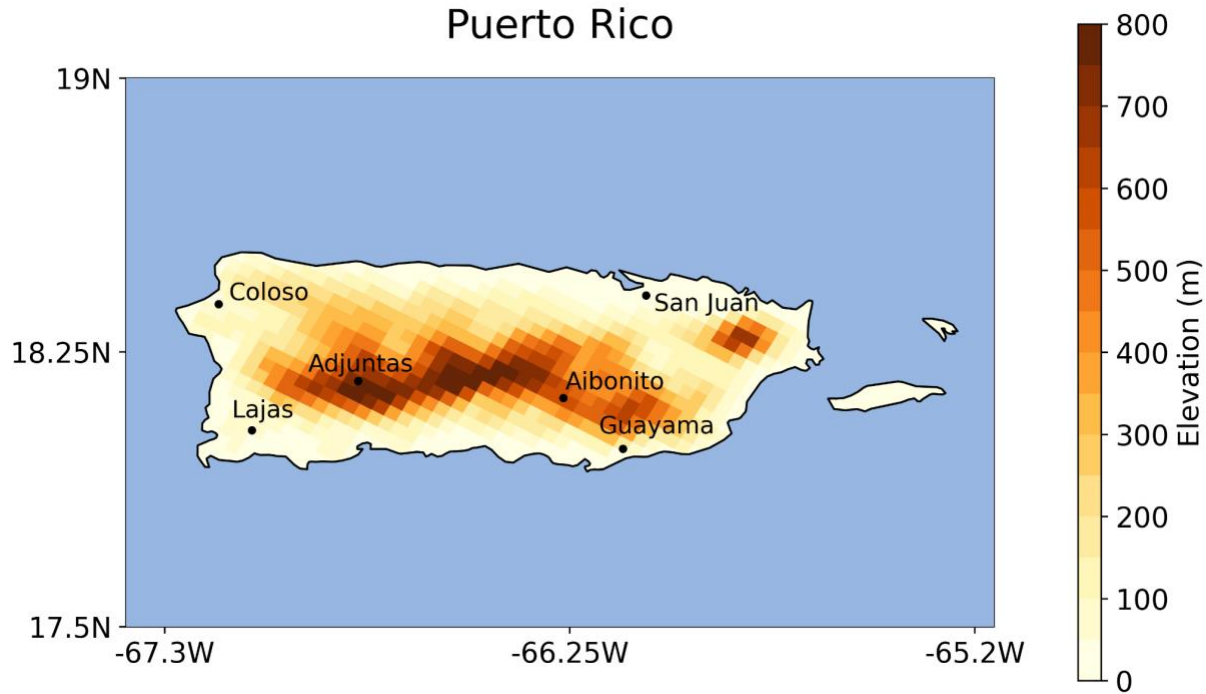


**Figure 1. Terrain map of Puerto Rico including elevation and sites of observation data used in this report.**

## 2 DATA

### 2.1 DAYMET VERSION 4

Daymet is a gridded estimate of daily weather parameters for North America, Hawaii, and Puerto Rico, developed by Oakridge National Laboratory (Thornton et al. 2022). The dataset covers the period from January 1, 1950, to December 31 of the most recent full calendar year for Puerto Rico. We choose Daymet because it is the only available gridded data product that provides high spatial and temporal resolutions (1-km daily data) over 70 years over Puerto Rico. The weather parameters include daily minimum and maximum near-surface air temperature, precipitation, vapor pressure, solar radiation, snow water equivalent, and day length. Of these, the main parameters used in this report are daily minimum and maximum surface air temperatures, precipitation, and incident shortwave radiation. The input data for Daymet were observations from ground-based meteorological stations available from the Global Historical Climatology Network-Daily dataset provided by the National Centers for Environmental Information (Menne et al. 2012). In locations with low station density, the latest algorithm of Daymet v4 dropped the iterative station density calculation and instead used a precalculated array of station distances to define a search radius for each estimation location which was sized to capture the average number of input stations. As such, Daymet is one of the few datasets that has a high-resolution estimate over low-station-density regions.

## 2.2 ERA5

ERA5 is a reanalysis dataset that combines vast amounts of historical data into global estimates using advanced modeling and assimilation systems. We use ERA5 due to its large amounts of weather variable and the high spatial and temporal resolution available over a long temporal period. The ERA5 dataset includes many weather variables on an hourly basis, on 37 pressure levels and at a spatial resolution of 30 km. It is potentially useful for examining large-scale climate forcings, although its coarseness does not capture the complex terrain and neglects the localized climate of the small island (compare Figure 2 and Figure 3). ERA5 land-only data has a higher resolution, 9 km, but excludes some coastal regions on the island.

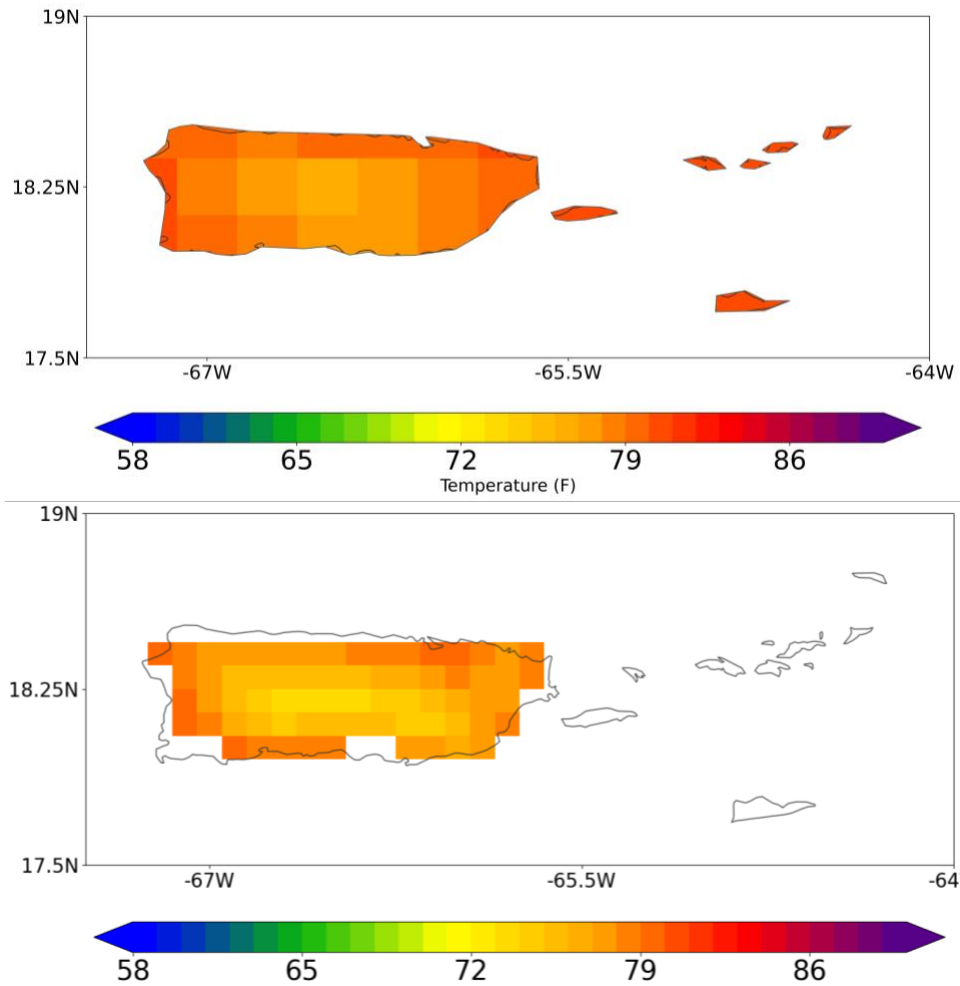


**Figure 2. 1950-2019 averaged fall air temperature using standard ERA5 atmosphere (spatial resolution: 30 km, top), and ERA5 land-only (spatial resolution: 9 km, bottom).**

## 2.3 STATION OBSERVATIONS

Station observations are local climate conditions taken from specific sites throughout Puerto Rico. We use these datasets as cross validations for Daymet because they are the actual climate conditions observed in the area—although there could be uncertainties in these observations. Monthly averaged station data were obtained through the National Weather Service National Oceanic and Atmospheric Administration. The data available varied depending on the site, but variables included were based on daily minimum, daily maximum, average near-surface air temperatures, precipitation, snowfall, snow depth, heating degree days, cooling degree days, and growing degree days. In this report, we used temperature and precipitation to cross validate the Daymet and ERA5 data products. We picked 12 sites to use, based on years of data available and the latitude and longitude information available. The sites had varying years of data available with San Juan going as far back as 1899. Precipitation values were available at all sites. Minimum and maximum temperature were available at 9 of the 12 sites. Note that the San Juan observation data is an average of the San Juan Metro area measurements, while the others were taken at each site’s location. Observation data were missing for some years and was not used in calculations.

## 3 METHOD

Monthly averages were calculated for each variable over all the years available. The data were grouped by seasons: winter (December, January, February), spring (March, April, May), summer (June, July, August), and fall (September, October, November). All calculations were done with respect to time over each latitude/longitude grid point. Linear regression was calculated at every pixel using the variable with respect to time. The formula used first calculated covariance along the time axis using:

$$cov = \frac{\sum_{n=1}^N (X_n - X_{\text{mean}}) * (Y_n - Y_{\text{mean}})}{N}$$

where  $X$  is the data being calculated with respect to, in this case time;  $Y$  is the data calculated, in this case the temperature, precipitation, and incident shortwave radiation; and  $N$  is the number of data points. Standard deviation ( $xstd$ ) of each variable was calculated using a built-in NumPy command along the time axis. Last, the slope of the linear regression (or the long-term trend) was calculated using covariance and standard deviation with formula:

$$slope = \frac{cov}{xstd^2}$$

The slope maps in Section 4 show the variable’s long-term trend in Fahrenheit/year, mm per day/year, and watts per square meter/year for temperature, precipitation, incident shortwave radiation, respectively. We also use 1950–1979 as a baseline, and compare with the most recent 30 years (1989–2019) to show the climate change impacts on each variable across Puerto Rico.

## 4 RESULTS

This section presents the seasonal averaged air temperature and precipitation; the seasonal averaged daily maximum air temperature for summer, spring, and fall; and the seasonal averaged

daily minimum air temperature for winter. Direct time series comparisons to station observation sites in the northwest, northeast, southwest, southeast, and two sites in the interior mountains (Figure 1) were also made for temperature and precipitation.

#### 4.1 TEMPERATURE

Figure 3 shows the seasonal mean air temperature, changes in seasonal mean air temperature from baseline (1950–1979) to the most recent 30 years (1989–2019), and the slope of linear regression of the seasonal mean air temperature over the past 70 years. It is apparent that the lowlands to the South and North are the hottest regions in Puerto Rico. The mountains in the interior can be up to 15°F cooler than the coast in the summer. Among the four seasons, summer and fall are the hottest, with the mean air temperature getting to about 84°F along the coast; winter is the coolest, with the mean air temperature getting to as low as 62°F in the interior. However, because Puerto Rico is located within the tropics, mean temperature does not have as much seasonal variability as in latitudes farther from the equator. All four seasons show warming trends, with the eastern and southwestern regions of the island warming more (1–2°F) than the central part (0.5–1°F) from early decades to the recent decades. The long-term trend is consistent with decadal changes in terms of the spatial variability of the temperature warming.

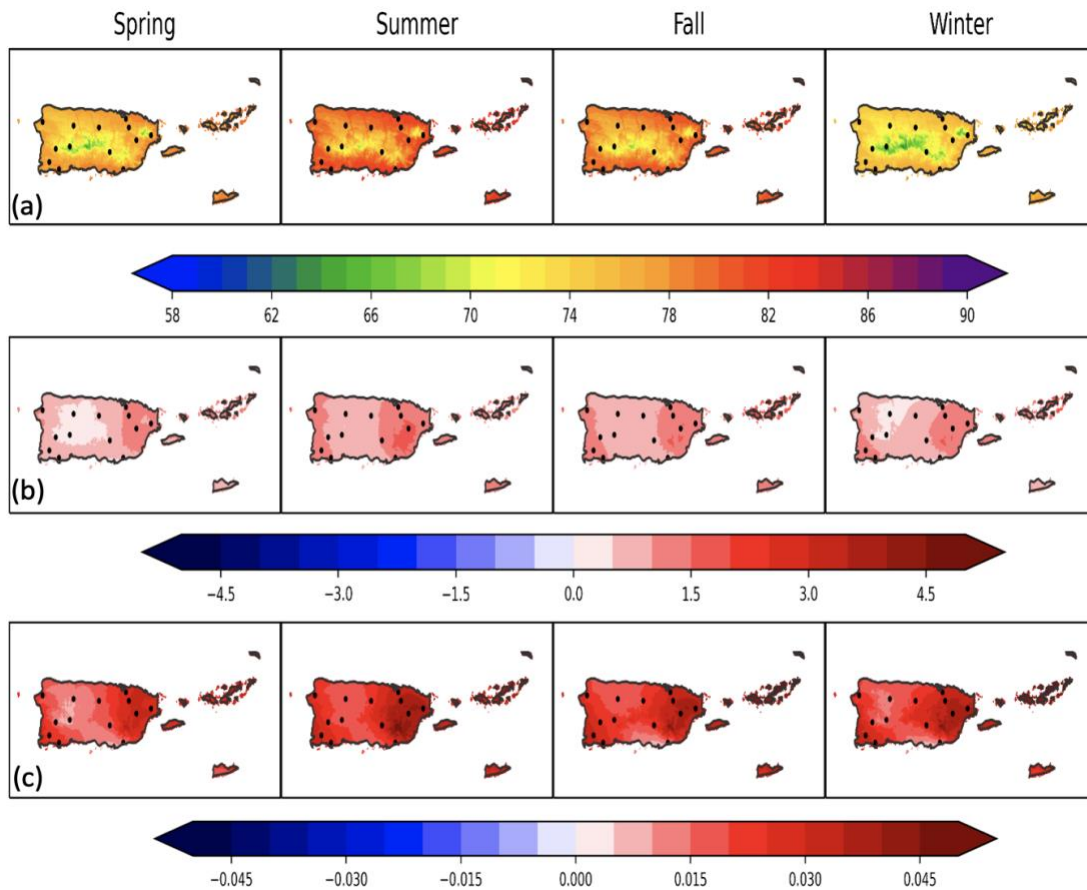


**Figure 3. (a) Seasonal mean temperature in Fahrenheit, 1950–2019. (b) Seasonal mean difference in Fahrenheit, 1989–2019 minus 1950–1979. (c) Long-term trend (or slope of linear regression) of seasonal mean temperature, 1950–2019.**

Figure 4 shows the seasonal mean daily maximum (minimum for winter) air temperature during the past 70 years, their changes from baseline to the most recent 30 years, and the long-term trend over the past 70 years. Among the four seasons, summer and fall are the hottest; mean daily maximum air temperature is in the 90s (°F) along the coast. Winter is the coolest: mean daily minimum air temperature is about 58°F in the interior. San Juan and Ponce, two heavily populated cities on different coastlines, are included in the areas of highest mean daily maximum air temperature. For the daily maximum air temperature, the warming is slightly weaker than that for seasonal mean, with 0.5–1.5 °F over east in summer and northeast in spring and fall. The changes in seasonal mean and daily maxima indicate that the air temperature distribution is not only shifting warmer, but also getting narrower. On the other hand, the Daymet data shows that the maximum air temperatures in summer to fall experience some cooling over the western regions, even to the southwest, where the seasonal mean was increasing. The area of greatest cooling is in the mountainous region with less station density, so the cooling over the western regions could have large uncertainties in the Daymet data product. The minimum air temperature in winter has warmed uniformly across the entire island, 1.5–3°F from early decades to recent decades over the eastern and southwestern coasts, and 1–1.5°F over the central island. The warming for the minimum winter air temperature is much stronger than that for the winter mean air temperature as well as the seasonal mean maximum temperature in the other three seasons throughout the entire island, consistent with findings of most of the North American continent (Zobel et al. 2017).

Overall, we see vast spatial variability in long-term trends across the entire island, calling for a very high-resolution dataset to investigate any climate change over Puerto Rico. Typical Earth System Model grids or moderate resolution of a Regional Climate Model grid are not sufficient for this purpose. San Juan, the most populous city in Puerto Rico, has one of the highest rates of temperature warming in all seasons. This trend continues to the region east above Humacao and as far as the islands. While Ponce has been less affected by the summer warming than San Juan, it has a slightly higher average maximum temperature than San Juan. Both of these highly populated cities have an average maximum temperature of ~90°F in the summer, which is worsened for their inhabitants by the humidity of the island.

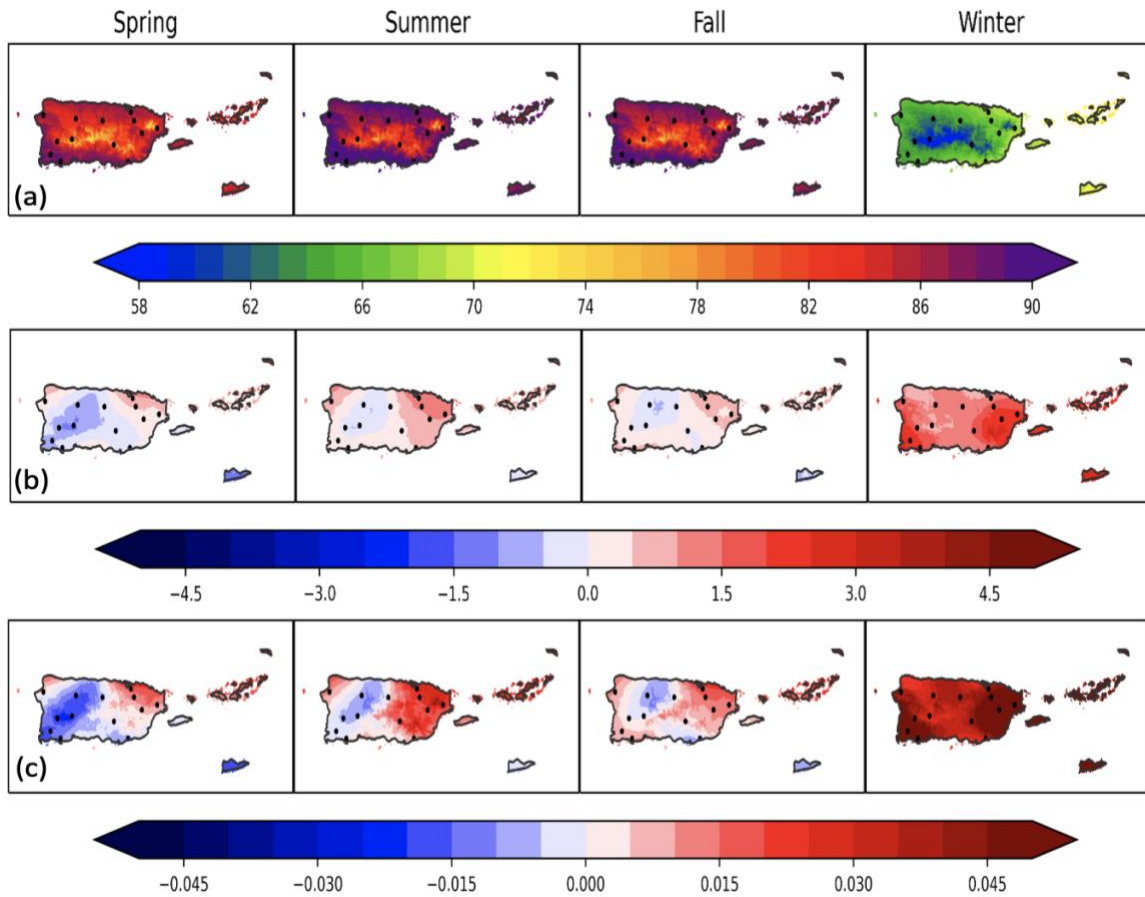


**Figure 4. (a) Seasonal average daily maximum air temperature in summer, spring, and fall, and daily minimum air temperature in winter. (b) Air temperature difference between 1989–2019 and 1950–1979 (1989–2019 minus 1950–1979) for seasonal average maximum of summer, spring, and fall and minimum of winter. (c) Long-term trend (or slope of linear regression) of seasonal maximum temperatures for summer, spring, and fall and seasonal minimum for winter, 1950–2019.**

Figure 5 compares Daymet and in-situ observations for summer (winter) mean and daily maximum (minimum) air temperature and their long-term trends based on linear regression using 70-year Daymet data and more than 100-year in-situ data over locations across the islands with various terrains and land uses. In general, the Daymet and in-situ data are quite close in terms of both long-term trends and temperature magnitudes, except for winter minimum air temperature. For example, both the summer mean air temperature and the daily maximum air temperature over the San Juan area are steadily increasing. Both winter mean and daily minimum air temperature are increasing; however, as mentioned, there is a discrepancy between in-situ observation and Daymet in daily minimum air temperature. For example, Daymet is 4°F lower than in-situ observations over the San Juan area. There are uncertainties in both datasets. However, we found that the Daymet data do not consider urban land use and its warming effect, which potentially the air temperature could be lower than observations. On the other hand, Daymet is 5–6°F higher than in-situ observation over Adjuntas, with the highest elevation over entire island, indicating that either the Daymet's grid spacing is still not fine enough or the algorithm in Daymet is not sufficient to capture the changes of air temperature of high elevations.

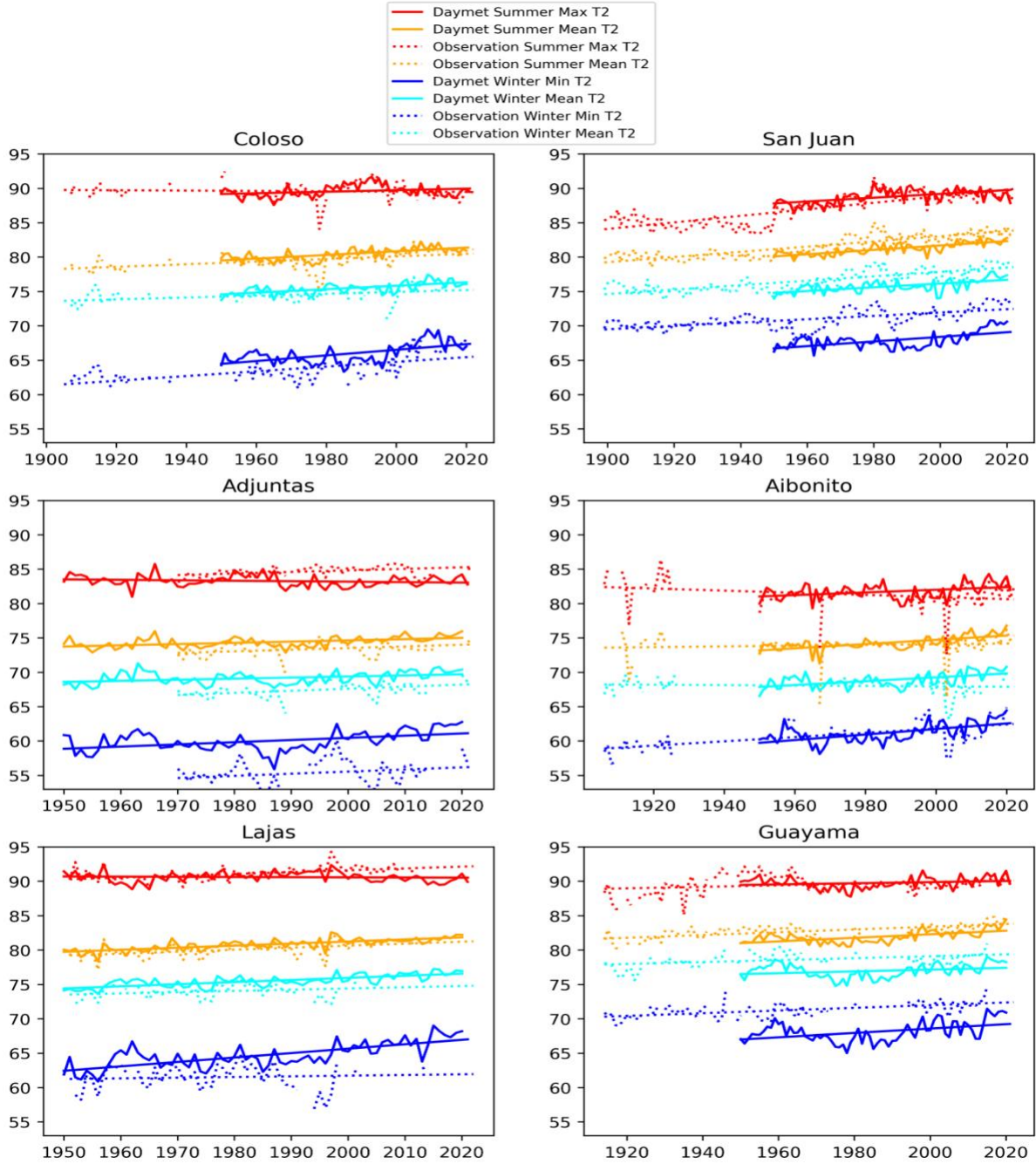


**Figure 5. Daymet and in-situ observed 2-m air temperature (in Fahrenheit) time-series in summer and winter over Coloso (Northwest), San Juan (Northeast), Lajas (Southwest), Guayama (Southeast), Adjuntas (western mountain), and Aibonito (eastern mountain). Solid lines are Daymet, dashed lines are in-situ observations.**

## 4.2 PRECIPITATION

Figure 6 shows seasonal precipitation, precipitation change from the baseline to the most recent three decades, and the 70-year-long trend in precipitation data in Daymet. From the geospatial pattern of seasonal mean precipitation (Figure 6a), we see that the majority of rain falls in El Yunque to the northeast in all seasons. Due to the steep mountains toward the southern interior, cities like Ponce get less than half of the rain compared other locations on the northern coast, which are exposed to northeastern trade winds. The trade winds bring moisture from the Atlantic that is favorable for the formation of rainfall (Richards et al. 2015; Gómez-Gómez et al. 2014).

All seasons have a similar spatial trend for magnitude of daily precipitation. Fall has the most rainfall compared with the other three seasons. Fall reaches just over an average 10 mm per day in El Yunque. The interior mountains and the majority of the island receive at least 6 mm per day. Fall is the only season with noticeably higher precipitation over the peaks of the western mountains. Winter has the least precipitation, with the majority of the island receiving less than 4 mm per day. El Yunque is the exception, reaching around 7 mm per day. Spring and summer have similar spatial patterns of precipitation, with summer having 1–2 mm more precipitation than spring in most regions. The exception is the south and southwest parts of the island where the minimum is about 2.5 mm per day.

Figures 6b and 6c show the change in precipitation from the early 20<sup>th</sup> century (baseline) to recent decades, as well as the long-term trend over the 70-year period. Over the majority of the island, summer precipitation has decreased by more than 20% over many locations, especially over the southern coast, which is already very dry compared with other parts of the island. There has also been a significant decrease in precipitation over both the western and eastern parts of the island. Given that most of the freshwater used for drinking, agriculture, and production of goods is found within rivers or aquifers, decreases in precipitation can be detrimental; precipitation is one of the main sources of replenishment (Gómez-Gómez et al. 2014). Compared with summer and winter, Fall and spring precipitation increases over last more than 70 years over the entire island. The only exception is in small regions below Mayaguez and Humacao, which show small decreases. We investigated the potential mechanisms for these precipitation changes across seasons by looking at atmospheric circulations, total column precipitable water, and sea level pressure (SLP) changes in Section 4.4.

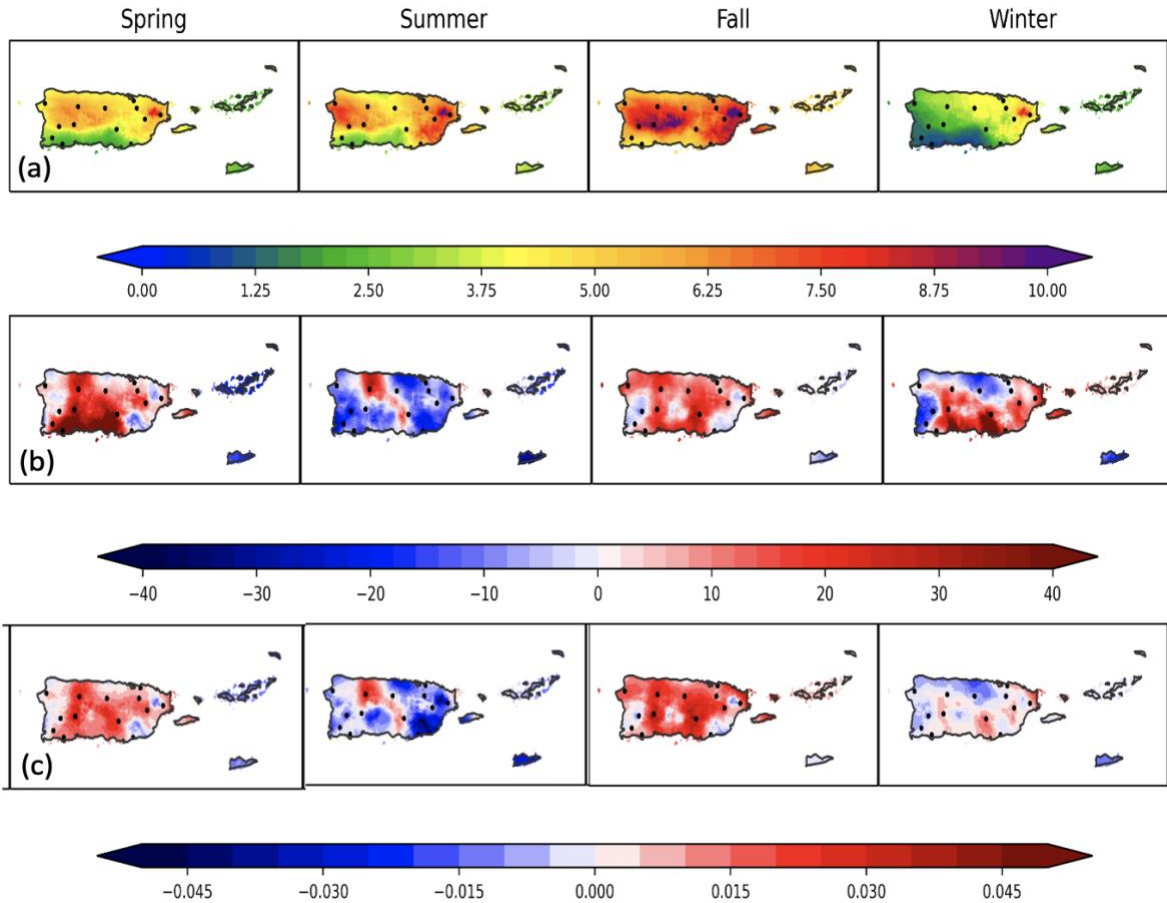


**Figure 6. Daymet precipitation data with observation sites. (a) Seasonal mean daily precipitation (mm/day), 1950–2019. (b) Seasonal percentage change of averaged daily precipitation, 1989–2019 minus 1950–1979. (c) Long-term trend (or slope of linear regression) of seasonal averaged daily precipitation, 1950–2019.**

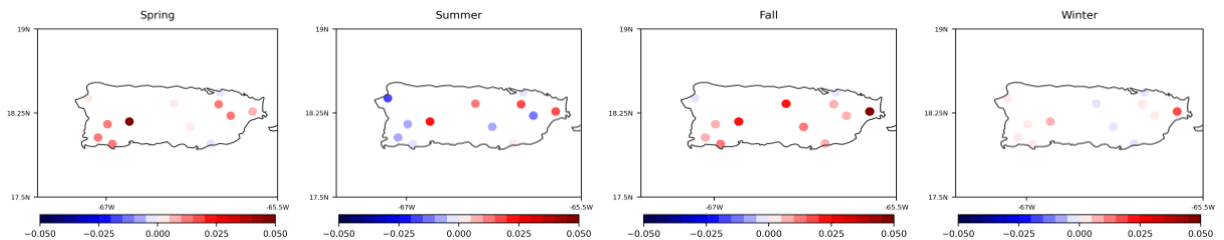


**Figure 7. Long-term trend (or slope of linear regression) of seasonal precipitation change with respect to year from 1950–2019 (mm/yr).**

To validate the Daymet precipitation data, Figure 7 shows the long-term trends of seasonal precipitation during 1950–2019 from station observations. Overall, the in-situ precipitation data shows a similar long-term trend to that seen in Daymet data, indicating that the Daymet data can reasonably capture the long-term trend and seasonal as well as spatial variabilities. For example,

there are overall increases in the fall and spring while decreases in summer; and winter has the lowest magnitude of changes.

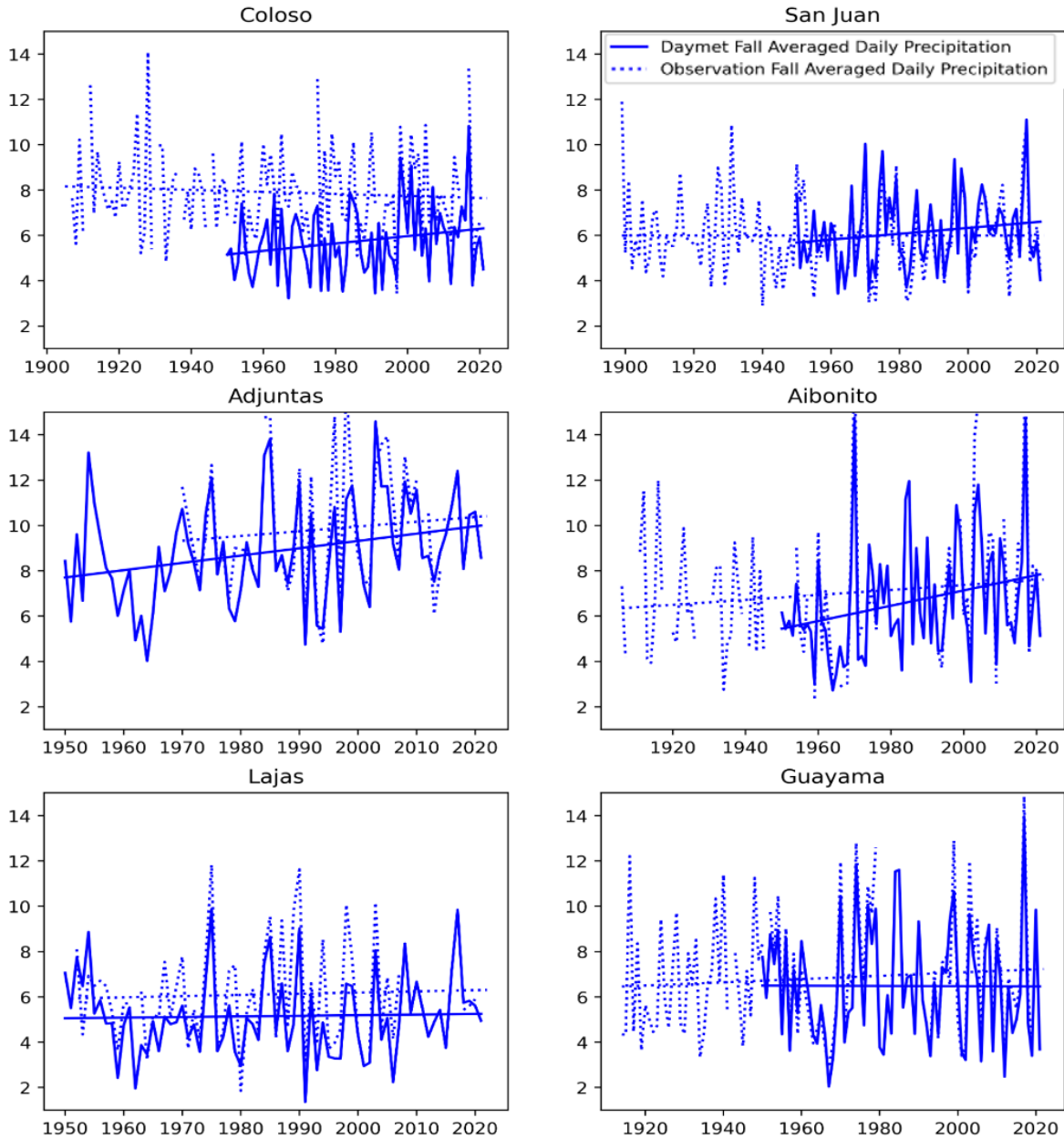


**Figure 8.** Time series of daily precipitation (in mm/day) for Coloso, San Juan area, Adjuntas, Aibonito, Lajas, and Guayama for fall (the wettest season) during 1950–2019 for Daymet and even longer time series for certain locations. Solid lines are based on Daymet data. Dashed lines are based on station observations.

Figure 8 compares the time series and long-term linear trend of the six locations shown in Figure 1 from in-situ observations and Daymet data. While the long-term trends do not specifically match over all the locations, Daymet still does a good job at estimating precipitation; it matches daily magnitudes and their temporal variabilities very well. Precipitation is a highly localized variable

and can vary greatly even within a small spatial area, and these values were taken at a specific latitude/longitude pair. Therefore, these results are encouraging because there are not many datasets available over Puerto Rico. The precipitation and the air temperature available in Daymet at such a high spatial and temporal resolutions can be very useful when evaluating climate change and its impacts on water resource and energy.

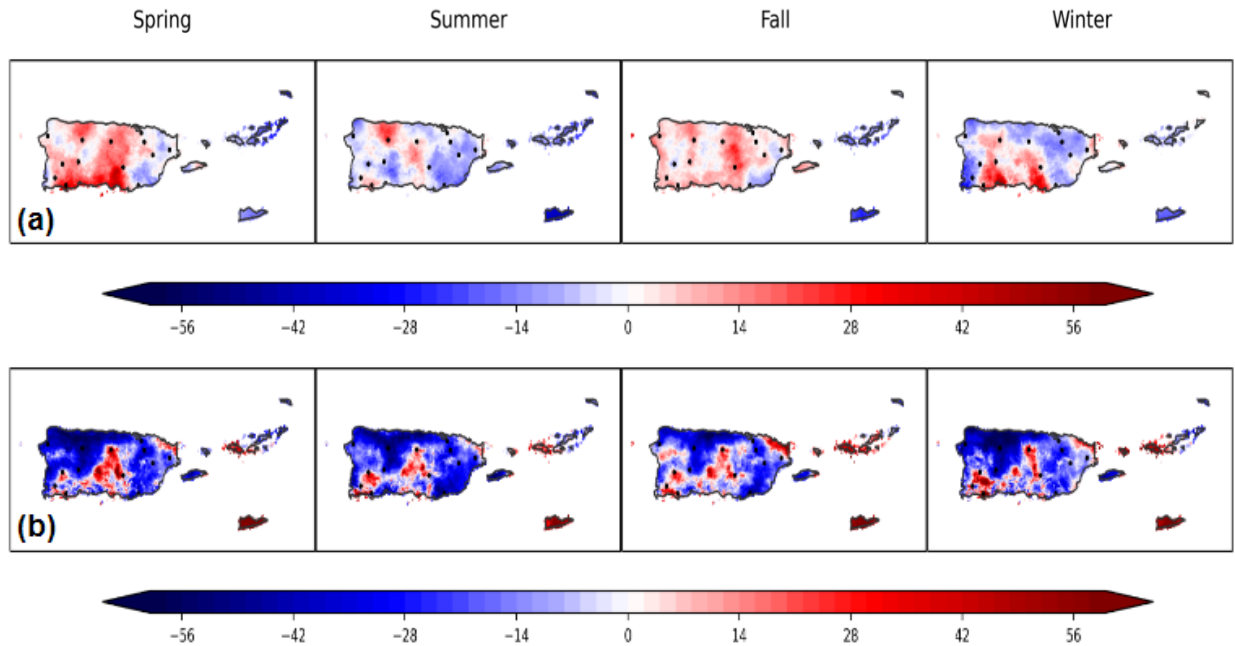


**Figure 9. Daymet extreme precipitation data with observation sites. (a) Percentage change of seasonal 95th percentile daily precipitation in 1950–1979 compared to 1989–2019. (b) Percentage change of seasonal 5th percentile daily precipitation in 1950–1979 compared to 1989–2019.**

To further illustrate the changes in precipitation, Figure 9 shows the changes in the 95th and 5th percentiles of each seasons' daily precipitation. To avoid an outsized influence from nonprecipitating days and days with drizzle, both percentiles were taken from daily data that had precipitation values of  $\geq 0.1$  mm per day. In general, we found that the spatial pattern of the changes in 95th percentile was very similar to that of mean changes. For example, there is a decrease in summer extreme precipitation and an increase in spring and fall precipitation over the majority of Puerto Rico. During the spring and fall, extreme rainfall greatly increases over most of the island, except over the southwest and El Yunque, where precipitation decreases by  $\sim 7\%$ . Precipitation in the El Yunque region is consistently high, but the 95th percentile and mean both decrease over the rainforest. The rest of the island experiences a 10–45% increase in 95th percentile precipitation during the spring. The largest increase is the island's southern coast, which receives the least daily precipitation. Fall has similar spatial trends: the 95th percentile increases by 6–20%, with the greatest increase over the central interior of the mountains. During the summer, precipitation decreases by 0–15% over most of Puerto Rico. There are localized areas of 14–20% increase in the Arecibo and central interior mountains. Winter experiences the greatest spatial differences in 95th percentile precipitation. The areas of increase between Lajas and Guayama extend into the

mountains to the north. These increases range from 14–35%. The rest of Puerto Rico shows a decrease of 5–20% during this time.

The changes in 5th percentile precipitation are spatially similar during all seasons. The central interior of the mountains, parts of the southwest, San Juan, and area to the east of San Juan are the only regions where precipitation increases, by around 20–40%. Precipitation in the rest of Puerto Rico show 20–60% decrease in all seasons. We also examined the days that exceed the baseline’s 95th percentile or days below the baseline’s 5th percentile, and found most days above or below the extremes occur in San Juan. The most urban site in San Juan had the greatest number of days that exceeded the extreme percentile threshold. This could indicate that, especially in urban areas, the wet days are getting wetter, and dry days are getting drier. There was not a clear long-term trend in the number of days that exceed the baseline’s 95th percentile. However, we do see an increasing trend through all seasons for the number of days below the 5th percentile, which indicates that more and more dry days are happening across the island.

### 4.3 SHORTWAVE RADIATION

Incident surface shortwave radiation can be roughly defined as solar energy with wavelengths in the range of 300–3000 nm that reach the Earth’s surface. The Daymet incident shortwave radiation flux density is an average over the daylight period of the day. Daymet uses the primary temperature and precipitation values to derive shortwave radiation and provides valuable data for examining changes and long-term trends. It can inform solar panel setting decisions, which will be useful in Puerto Rico’s planned transition to solar energy. There is no radiation data available from in situ observations over Puerto Rico, so we were not able to validate the Daymet radiation data.

As shown in Figure 10a, Daymet presents the seasonal variability of solar radiation, with spring and summer having larger incident shortwave radiation than fall and winter. Spatially, the highest incident shortwave radiation is in the southwestern region of the island, and the lowest is in the east near El Yunque. This geospatial pattern correlates well with the spatial pattern of precipitation. Increased clouds within the region would reflect more of the radiation away from the land surface. For example, El Yunque has the highest precipitation year round, but the lowest shortwave radiation. On the other hand, on the southwestern and southern coast there was little rain year round, which led to higher incident radiation. However, the change in incident shortwave radiation, as shown in Figure 10b, decreased in every season from baseline to the most recent decades. There was a larger decrease in spring and fall, possibly due to the precipitation increase in these two seasons. Note that even though the incident radiation is lower in the east and in cool seasons, the values still are near 300 watts/meter<sup>2</sup>. This is the average over each daylight hour in a day, which computes to approximately 3,000 watts/meter<sup>2</sup> throughout the day for each square meter. For reference, it takes about 350 watts to drive an electric vehicle a mile, so a day of solar radiation can provide power for ~8.5 miles of driving.

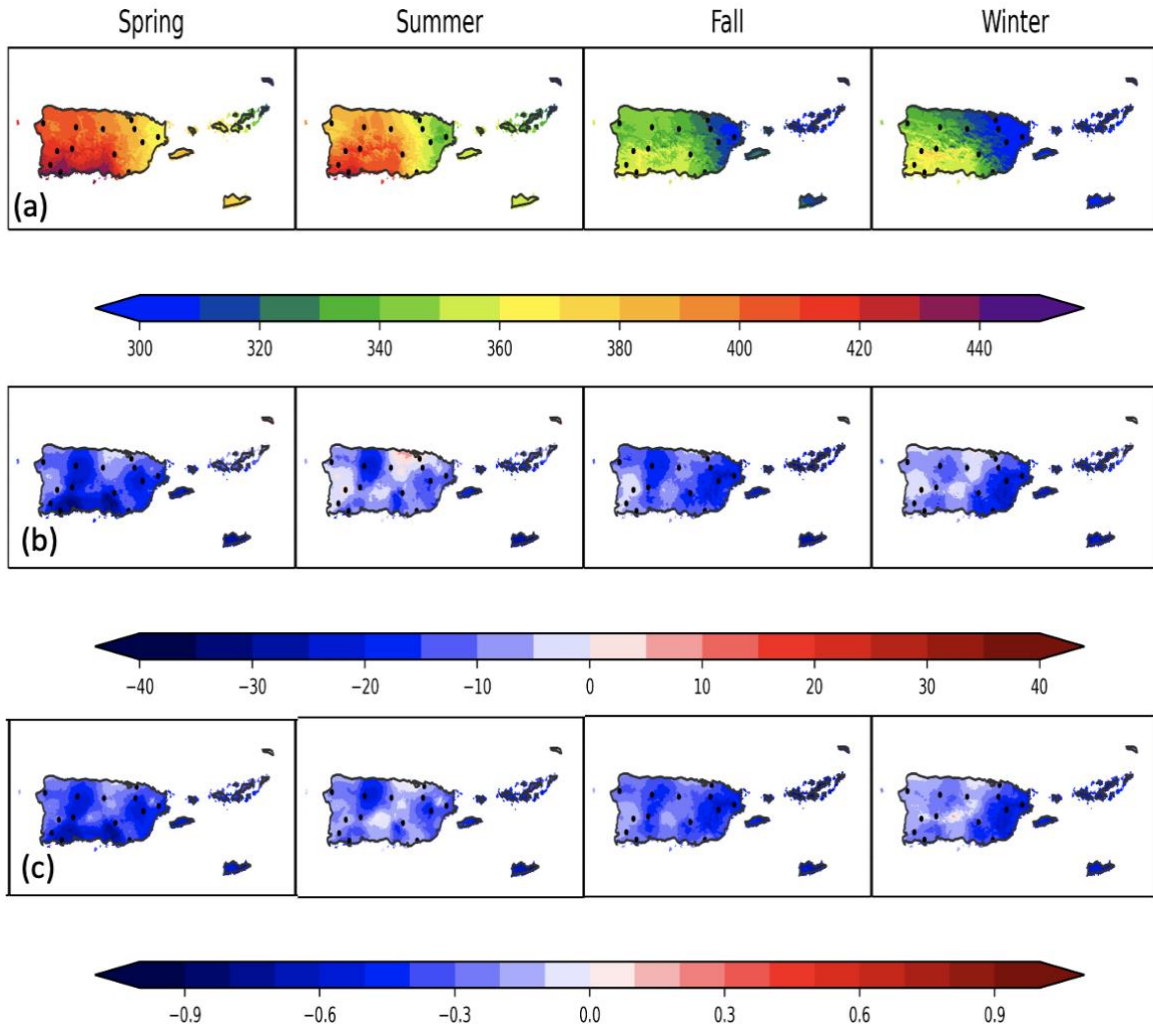


**Figure 10. Daymet shortwave radiation data with observation sites: (a) Seasonal mean incident shortwave radiation in  $\text{W/m}^2$  per daylight hour, 1950–2019. (b) Seasonal difference of shortwave radiation in  $\text{W/m}^2$ , 1989–2019 minus 1950–1979. (c) Long-term trend of seasonal shortwave radiation, 1950–2019.**

#### 4.4 LARGE-SCALE METEOROLOGICAL CONDITIONS

Large-scale weather parameters such as trade winds, total column rainwater (TCRW), SLP, and total cloud cover were examined using the ERA5 dataset. The average of the available ERA5 data was taken from the 1959–2019 time period. The difference was computed between the 1990–2019 and 1959–1989 time periods to investigate any large-scale condition changes within the past 60 years. SLP shows increases in summer and winter, and a decrease in fall, promoting precipitation increase over Puerto Rico and the Caribbean islands during the fall. The total cloud cover is increasing over Puerto Rico in every season, especially summer and fall. This might be associated with the decrease of the incident solar radiation.

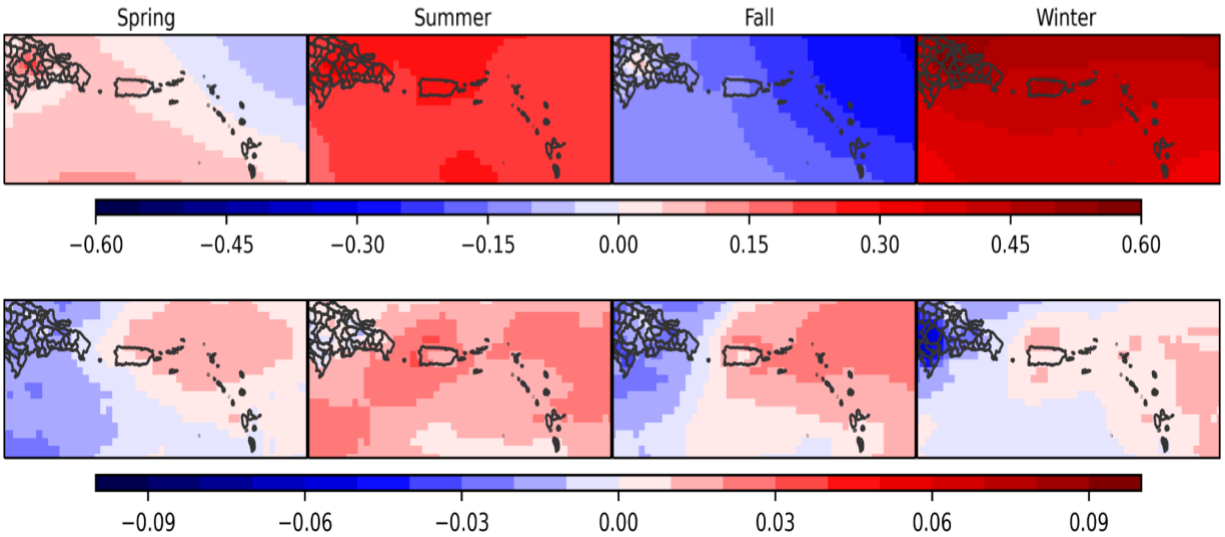


**Figure 11. Top: Changes in ERA5 monthly averaged SLP. Bottom: Changes in total cloud cover. Changes are calculated using the 1999–2019 average minus the 1959–1979 average.**

Figure 12 shows the seasonality of and changes in TCRW over the past 60 years. First of all, fall receives the largest amount of TCRW compared to other seasons across the region we examined, including Puerto Rico and surrounding islands. There is particularly high TCRW over the east coast of Puerto Rico, consistent with the highest precipitation in the fall. TCRW also shows a clear difference between land and sea: TCRW is higher over islands than over sea. This could be due to the winds shown in Figure 13. The Puerto Rican mountains block and accumulate the moisture brought by the trade winds. Interestingly enough, TCRW also increases more in fall than in the other three seasons. The next-highest increase is in the spring, consistent with the precipitation increase shown in Figures 6b and 6c. This provides a moisture source for precipitation development.

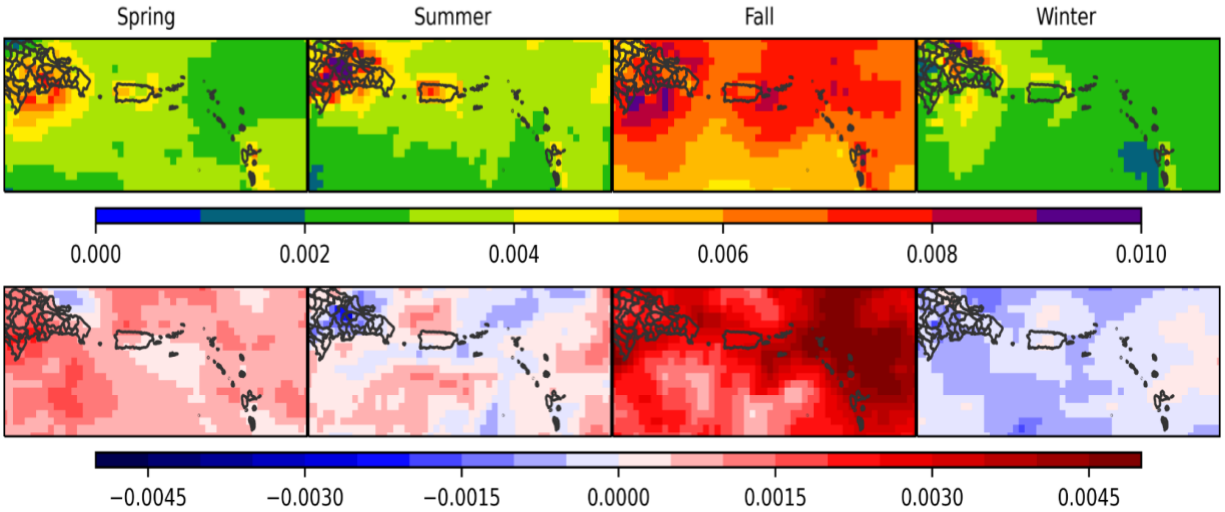


**Figure 12. ERA5 monthly averaged TCRW. Top: Average monthly TCRW in  $\text{kg/m}^2$  from 1959–2019. Bottom: Changes in monthly averaged TCRW, 1999–2019 average minus 1959–1979 average.**

While we see decreases in SLP and an increase in TCRW, particularly in the fall, it is important to investigate the circulations and their changes because they provide dynamic forcing to develop precipitation. Figure 13a shows persistent trade winds: easterly winds that blow across the North Atlantic, bringing moisture to Puerto Rico. The trade winds originate near the North Pole, so they tend to be stronger in the winter and weaker in the summer. Trade wind intensity has an inverse effect on precipitation potential: the stronger the winds are, the more the sea is disrupted, mixing cool and warm water, which is less favorable for precipitation development. On the other hand, weaker trade winds allow the warm water near sea surface to be brought into the islands. This also explains the higher magnitudes of precipitation in the summer and fall compared to winter and, to a lesser extent, spring. However, the direction of the winds remains important for moisture to be brought to the islands. Because the trade winds arrive in Puerto Rico from the northeast, the mountains create a rain shadow for the southern coast of the island.

Figure 13b shows the changes in these winds during each season for the past 60 years. We found that fall showed a cyclonic circulation in the wind pattern changes (1999–2019 averages minus 1959–1979 averages), bringing moisture from the northern Atlantic to Puerto Rico. This is favorable for convergence and increased precipitation (Figure 6b, 6c). Spring shows the same change in wind pattern, but to a lesser extent. This explains the spring increase in rain, along with the increase in precipitable water (Figure 12). Summer and winter, on the other hand, do not show the cyclonic circulation. Instead, there might be an anti-cyclone in the north of the domain shown in Figure 13. The wind speed is becoming much stronger in winter, intensifying the ocean mixing between cool and warm water. Therefore, these conditions are not favorable for the development of precipitation.

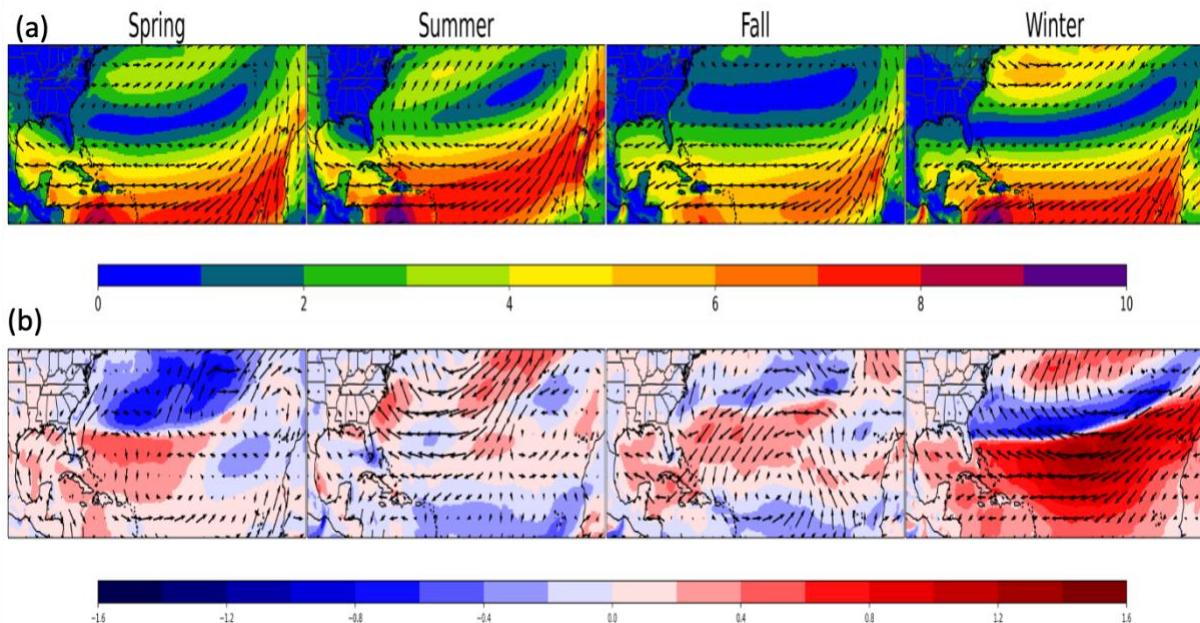


**Figure 13. (a) ERA5 seasonally averaged 10-m wind speeds (contours) and directions (arrows), 1959–2019. (b) Changes in winds in each season, 1959–1979 compared to 1999–2019 (1999–2019 minus 1959–1979).**

## 4.5 LOCAL-SCALE LAND COVER CHANGES

Puerto Rico is home to large amount of urban sprawl (Homer et al. 2004). The urban land cover area is expanding quickly, but the population density in this area is low. Based on Kennaway et al. (2007), urban and developed areas have increased 795% from 1951 to 2001. This land cover includes military and naval reserves, nonproductive land, and highly developed urban land cover. Puerto Rico has continued to grow in population since 2001, but more recent land cover data is currently unavailable. Urban land cover absorbs and retains much more heat than other types of land cover. This can cause effects such as urban heat islanding and urban pollution islanding, which increase the local temperatures and air pollutants in urban areas (Li et al. 2018). These combined warming effects from global and local scale (Figure 4) in all seasons over the northeast coast and San Juan area increase the threat of higher pollution, heat-related health issues, and higher energy costs. Urbanization can also have significant impacts on precipitation through various mechanisms. It can either enhance or reduce precipitation amounts or change precipitation spatial patterns, depending on the physical areas and the precipitation types being studied, as well as the definition of urban versus rural areas (Lin et al. 2021; Song et al. 2021; Li et al. 2023).

## 5 SUMMARY AND DISCUSSION

Puerto Rico is still in recovery years after being hit by devastating tropical storms such as Hurricane Maria in 2017. The lack of renewable energy in particular worsen the impacts of anthropogenic induced climate change on the island, and leave it vulnerable if another extreme storm occurs there. Thus, it is important to investigate how the climate in Puerto Rico has already changed in observable history to inform transition to renewable energy. Our study revealed that temperatures have already increased as much as a few degrees over the past seven decades within areas such as the land between San Juan and Humacao. Mean temperature has increased throughout the entire island, especially in fall and summer, which were already the hottest months. Summer had the highest rate of warming out of all seasons: temperatures increased by 1–2°F throughout all of Puerto Rico in these months. Maximum temperature has increased in every season in all of the island's urban areas. The average maximum temperature, which was already in the range of 90–100°F has increased by a degree in cities like San Juan. This poses a threat to the population, which is exposed to long periods of intense heat. Minimum temperature increased at an even higher rate than mean and maximum air temperature throughout all of Puerto Rico for every season, especially in winter, which indicates that the islands are experiencing shorter winters and longer summers under global warming. Rapid urban sprawl is another reason that caused a greater temperature increase.

Changes in precipitation over time have been less straightforward. In general, we see decreased precipitation in summer and increased precipitation in spring and fall. This increase in rainfall is caused by decreases in SLP, increases of precipitable water, and increases in the cyclonic circulations brought by the trade winds. These changes in seasonal mean precipitation are mostly due to the contributions from extreme precipitation (95<sup>th</sup> percentile and higher). On the other hand, there was also an increase in the number of very dry days (precipitation less than 5<sup>th</sup> percentile) over the past seven decades in all seasons over most regions. Incident shortwave radiation was highest in the spring, followed by summer. Even winter values are not necessarily low, as the tropics tend to get more sunlight than latitudes farther from the equator. These values showed a

decrease in every season, as the total cloud cover increased. While this is not favorable for solar renewable energy, the values were still large.

Our study benefits significantly from Daymet data. Although Daymet only provides an estimate of a few weather parameters, these provide a closer look at the Puerto Rican climate at a high resolution that captures its complex terrain that is often overlooked. In addition, there is often no instrumentation within certain regions to capture these near-surface meteorological variables, so the Daymet data was very helpful. Daymet appears to show a consistent trend and magnitude with real-world climate data over most of the locations examined.

## 6 ACKNOWLEDGEMENTS

This effort was supported through the Puerto Rico Grid Resilience and Transitions to 100% Renewable Energy Study (PR100), an initiative funded by the Federal Emergency Management Agency through an interagency agreement with the US Department of Energy. We thank Dr. John Hummel from Decision and Infrastructure Sciences division at Argonne for his review and constructive comments. The Xarray and NumPy packages were used to read the data files and calculations. The Cartopy and Matplotlib packages were used to map the results.

## 7 DATA AVAILABILITY

Daymet is a dataset derived from interpolation and extrapolation of daily meteorological observations (<https://doi.org/10.3334/ORNLDAAAC/2129>)

Monthly averaged station data was obtained through the National Weather Service National Oceanic and Atmospheric Administration (<https://www.weather.gov/wrh/Climate?wfo=sju>).

## 8 REFERENCES

Bhatia, K.T., Vecchi, G.A., Knutson, T.R. et al. 2019, “Recent increases in tropical cyclone intensification rates”. *Nature Communication* 10, 635. <https://doi.org/10.1038/s41467-019-08471-z>

Fordham, D.A., and B.W. Brook, 2010, “Why tropical island endemics are acutely susceptible to global change,” *Biodiversity and Conservation* 19:329–342. <https://doi.org/10.1007/s10531-008-9529-7>.

Gómez-Gómez, F., J. Rodríguez-Martínez, and M. Santiago, 2014, *Hydrogeology of Puerto Rico and the outlying islands of Vieques, Culebra, and Mona*, Scientific Investigations Map 3296, U.S. Department of the Interior and U.S. Geological Survey. Prepared in cooperation with the Commonwealth of Puerto Rico. DOI: <https://pubs.usgs.gov/sim/3296/pdf/sim3296.pdf>.

Gensini, V.A., A.M. Haberlie, and W.S. Ashley, 2023, “Convection-permitting simulations of historical and possible future climate over the contiguous United States,” *Climate Dynamics* 60(1-2):109–126. <https://doi.org/10.1007/s00382-022-06306-0>

Homer, C.G., C. Huang, L. Yang, B.K. Wylie, and M.J. Coan, 2004, "Development of a 2001 National Land Cover Database for the United States," *Photogrammetric Engineering and Remote Sensing* 70(7):829–840. <https://doi.org/10.14358/PERS.70.7.829>.

Hersbach, H., Bell, B., Berrisford, P., Biavati, G., Horányi, A., Muñoz Sabater, J., Nicolas, J., Peubey, C., Radu, R., Rozum, I., Schepers, D., Simmons, A., Soci, C., Dee, D., Thépaut, J.-N. (2023): ERA5 hourly data on single levels from 1940 to present. Copernicus Climate Change Service (C3S) Climate Data Store (CDS), DOI: [10.24381/cds.adbb2d47](https://doi.org/10.24381/cds.adbb2d47)

Kang, N.Y., Elsner, J. Trade-off between intensity and frequency of global tropical cyclones. *Nature Climate Change* 5, 661–664 (2015). <https://doi.org/10.1038/nclimate2646>

Kennaway, T., and E. Helmer, 2007, "The Forest Types and Ages Cleared for Land Development in Puerto Rico," *GIScience & Remote Sensing* 44:356–382. DOI:10.2747/1548-1603.44.4.356.

Liu, C., K. Ikeda, R. Rasmussen, M. Barlage, A.J. Newman, A.F. Prein, Chen, F., Chen, L., Clark, M., Dai, A., Dudhia J., Eidhammer, T., Gochis, D., Gutmann, E., Karkute, S., Li, Y., Thompson, G., and D. Yates, 2017, "Continental-scale convection-permitting modeling of the current and future climate of North America," *Climate Dynamics* 49:71–95. <https://doi.org/10.1007/s00382-016-3327-9>

Li, H., F. Meier, X. Lee, T. Chakraborty, J. Liu, M. Schaap, and S. Sodoudi, 2018, "Interaction between urban heat island and urban pollution island during summer in Berlin," *Science of the Total Environment* 636:818–828. doi: 10.1016/j.scitotenv.2018.04.254.

Li, C., Gu, X., Slater, L. J., Liu, J., Li, J., Zhang, X., & Kong, D. 2023, "Urbanization-induced increases in heavy precipitation are magnified by moist heatwaves in an urban agglomeration of East China". *Journal of Climate*, 36(2), 693-709.

Lin, Y., Fan, J., Jeong, J. H., Zhang, Y., Homeyer, C. R., & Wang, J. 2021, "Urbanization-induced land and aerosol impacts on storm propagation and hail characteristics". *Journal of the Atmospheric Sciences*, 78(3), 925-947.

Mearns, Linda; McGinnis, Seth; Korytina, Daniel; Arritt, Raymond; Biner, Sebastien; Bukovsky, Melissa; Chang, Hsin-I; Christensen, Ole; Herzmann, Daryl; Jiao, Yanjun; Kharin, Slava; Lazare, Michael; Nikulin, Grigory; Qian, Minwei; Scinocca, John; Winger, Katja; Castro, Chris; Frigon, Anne; Gutowski, William, 2017, The NA-CORDEX dataset, version 1.0. NCAR Climate Data Gateway, Boulder CO. Accessed June 1, 2020. <https://doi.org/10.5065/D6SJ1JCH>

Menne, Matthew J., Imke Durre, Bryant Korzeniewski, Shelley McNeill, Kristy Thomas, Xungang Yin, Steven Anthony, Ron Ray, Russell S. Vose, Byron E. Gleason, and Tamara G. Houston (2012): Global Historical Climatology Network - Daily (GHCN-Daily), Version 3. NOAA National Climatic Data Center. doi:10.7289/V5D21VHZ.

Pasch, R.J., A.B. Penny, and R. Berg, 2023, *National Hurricane Center Tropical Cyclone Report: Hurricane Maria*, January 4. [https://www.nhc.noaa.gov/data/tcr/AL152017\\_Maria.pdf](https://www.nhc.noaa.gov/data/tcr/AL152017_Maria.pdf)

Pokhrel, R., del Cos, S., Rincon, J. P. M., Glenn, E., & González, J. E. 2021, “Observation and modeling of Hurricane Maria for damage assessment”. *Weather and Climate Extremes*, 33, 100331. <https://doi.org/10.1016/j.wace.2021.100331>

Ramos-Scharrón, C.E., C.T. Garnett, and E.Y. Arima, 2021, “A Catalogue of Tropical Cyclone Induced Instantaneous Peak Flows Recorded in Puerto Rico and a Comparison with the World’s Maxima,” *Hydrology* 8(2):84. <https://doi.org/10.3390/hydrology8020084>

Richards, R.T., A. Emiliano, and R. Mendez-Tejeda, 2015, “The Effects of the Trade Winds on the Distribution of Relative Humidity and the Diurnal Air Temperature Cycle on Oceanic Tropical Islands,” *Journal of Earth Science & Climatic Change* 6:288. DOI: 10.4172/2157-7617.1000288.

Singh, S., & Bainsla, N.K. (2015). Analysis of Climate Change Impacts and their Mitigation Strategies on Vegetable Sector in Tropical Islands of Andaman and Nicobar Islands, India. *Journal of Horticulture*, 2, 1-5.

Song, X., Y. Mo, Y. Xuan, Q.J. Wang, W. Wu, J. Zhang, and X. Zou, 2021, “Impacts of urbanization on precipitation patterns in the greater Beijing–Tianjin–Hebei metropolitan region in northern China,” *Environmental Research Letters* 16(1):014042.

Thornton, M.M., R. Shrestha, Y. Wei, P.E. Thornton, S-C. Kao, and B.E. Wilson, 2022, Daymet: Daily Surface Weather Data on a 1-km Grid for North America, Version 4 R1. ORNL DAAC, Oak Ridge, Tennessee, USA. <https://doi.org/10.3334/ORNLDAAC/2129>

Zobel, Z., J. Wang, D.J. Wuebbles, and V.R. Kotamarthi, 2017, “High Resolution Dynamical Downscaling Ensemble Projections of Future Extreme Temperature Distributions for the United States,” *Earth’s Future* 5(12):1234–1251. <https://doi.org/10.1002/2017EF000642>



## **Environmental Science Division and Decision and Information Science**

Argonne National Laboratory  
9700 South Cass Avenue  
Lemont, IL 60439

[www.anl.gov](http://www.anl.gov)



Argonne National Laboratory is a U.S. Department of Energy laboratory managed by UChicago Argonne, LLC